AAS 19-928

AUTONOMOUS SATELLITE NAVIGATION USING INTERSATELLITE LASER COMMUNICATIONS

Pratik K. Davé[*] and Kerri Cahoy[†]

This work investigates the use of laser communication (lasercom) intersatellite links to obtain relative position measurements for autonomous navigation. Lasercom crosslinks have the potential to provide intersatellite range and bearing measurements in order to accurately navigate satellites in a wide set of orbit cases, including GNSS-denied, GNSS-limited, and deep-space environments. Numerical simulations are used to compare the lasercom crosslink approach with traditional positioning and navigation methods in example application cases in low Earth-orbit (LEO), geostationary Earth-orbit (GEO), highly elliptical orbit (HEO), and a Mars-orbiting constellation. The use of lasercom measurements in Earth-orbit results in errors on the order of 2 meters in LEO, 10 meters in GEO, and 50 meters in HEO, which is on-par with current GNSS-based navigation errors. A constellation of Mars-orbiters using the proposed navigation method results in 10-meter position errors, which is on-par with current DSN-based navigation errors, when DSN operations are available, and better than propagated state knowledge during DSN data gaps. Use of intersatellite lasercom systems for orbit determination also decreases dependence on ground-based tracking and navigation systems, enabling greater autonomy in space missions.

INTRODUCTION

The satellite industry is experiencing a trend towards smaller, less expensive spacecraft that benefit from lower launch costs. This motivates new distributed satellite architectures that must overcome operational challenges. Without significant increases in staffing and infrastructure, spacecraft operations typically performed by ground-based systems, like satellite navigation, will become overwhelmed as the number of operational satellites increases. While Global Navigation Satellite Systems (GNSS) perform well for spacecraft within its service volume, it provides only limited capability for missions at high altitudes and in highly-elliptical orbits (HEO), and cannot support deep-space science and exploration missions, such as those orbiting the moon or Mars.

The current standard for deep-space navigation outside of near-Earth orbit is collecting and processing orbits from ground-based radiometric data collected by the Deep Space Network (DSN). However, it is well known that this capability is limited by operational and geometric constraints. For example, there are large data-gaps on the order of one day for Mars orbiters.[1] Improved spatial and temporal navigation is critical for future human and robotic missions on the

[*] Doctoral Candidate, Department of Aeronautics and Astronautics, Massachusetts Institute of Technology, 77 Massachusetts Avenue, Cambridge, Massachusetts 02139, USA.
[†] Associate Professor, Department of Aeronautics and Astronautics, Massachusetts Institute of Technology, 77 Massachusetts Avenue, Cambridge, Massachusetts 02139, USA.

moon, Mars, and beyond. In an effort to address this need, we propose a new method of satellite navigation using intersatellite measurements from laser communication (lasercom) crosslinks in distributed satellite systems.

BACKGROUND

Autonomous navigation methods serve as a means to mitigate reliance on ground-based systems by utilizing some combination of on-board sensors that can measure relative range or bearing to known references independent of operator command. Several methods have been proposed, like those based on visual landmarks,[2] magnetic fields,[3] and atmospheric drag.[4] However, many of these methods are limited to low altitudes or specific orbit cases. GNSS-based navigation is the current state-of-the-art for autonomous navigation around Earth, though its performance is significantly limited outside of its primary service volume, from the surface up to 3000 km altitude. Navigation methods intended for deep-space applications, such as optical navigation[5] and pulsar navigation,[6] require dedicated instruments that may exceed the size, weight, and power (SWaP) constraints in small satellites, and also require sufficient identification and characterization of celestial references in order to achieve greater positioning accuracy. A more precise autonomous navigation method is needed for use in GNSS-denied, GNSS-limited, and deep-space environments.

One potential method to address this gap uses intersatellite data, or direct observations of the relative position vector from one satellite to another, to estimate the orbital positions of both spacecraft simultaneously.[7] Multiple measurements are used to capture the intersatellite data, typically by using different instruments. A radio or laser time-of-flight measurement is conventionally used to capture the range, or the magnitude component of the relative position vector. The directional component, or the bearing, is traditionally measured using a visual sensor, such as an optical telescope, and referenced to the inertial frame using an on-board attitude sensor, such as a star tracker. A time-series of intersatellite range and bearing measurements can then be fed into an orbital dynamics estimator in order to determine the position and velocity states of both spacecraft.[8]

This intersatellite method has the potential to leverage connectivity of satellites in a constellation or other distributed architecture for autonomous navigation, and be used at any altitude, in Earth-orbit and beyond. However, the ability to measure intersatellite bearing over long distances has traditionally been a challenge, resulting in this method largely being limited to spacecraft in the same or similar orbits.[7-11] Visual sensors can be limited by observability constraints, such as the minimum size, brightness, and resolution needed for proper detection, which effectively limits where the other spacecraft can be located relative to the sensor, both in range and direction.[10] For this reason, several studies using the intersatellite method limit their analyses to satellite orbits with small separations.[8-11] In order to analyze orbital cases of larger separations, other studies attempt range-only estimation without any bearing measurements.[12,13] Another limitation in the majority of previous studies is the use of radio-frequency (RF) sensors to measure intersatellite range,[7, 9-13] which are limited in precision compared to sensors operating at optical frequencies. In the present work, we show that the proposed concept of using lasercom crosslinks can improve upon these performance limitations by using the greater frequency bandwidth and narrower beamwidth of optical frequencies, thus enabling use of the intersatellite method over longer distances in connected and distributed satellite architectures.

APPROACH

Navigation using Lasercom Crosslinks

Satellite orbit determination methods involve the use of instruments to track and collect a time-series of measurements of the satellite's orbital trajectory. Measurements are then processed in a filtering algorithm to estimate the six-element state of the satellite, in the form of either classical Keplerian elements (a, e, i, ω, Ω, θ) or 3-dimensional position and velocity (x, y, z, $\dot{x}$, $\dot{y}$, $\dot{z}$), at a given epoch time, t. The measurement utilized in the intersatellite navigation method is the relative position vector between two satellites, referenced to inertial space.[7] Relative position vector can be derived from its magnitude and directional components, which translate to measurements of intersatellite range and bearing, respectively. In order to measure intersatellite range and bearing between satellites in a constellation, we propose using lasercom crosslinks.

Time-of-flight ranging measurements can be captured using time-embedded signals over communications links. Laser communications payloads operate at optical wavelengths with greater frequency bandwidth than RF systems. The higher bandwidth enables lasercom systems to measure range between two terminals with more precise resolution. RF systems typically achieve meter-level ranging precision; lasercom systems can achieve centimeter-level precision. The current state-of-the-art performance in satellite lasercom ranging was demonstrated to about 1-cm precision in one-way links from Earth to lunar orbit during the Lunar Laser Communication Demonstration (LLCD) mission in 2015,[14] however this was a ground-to-satellite demonstration, not satellite-to-satellite as intended for autonomous navigation using the intersatellite method.

Lasercom systems have narrow, sub-degree beamwidths compared to radio-frequency (RF) systems. In order to point the narrow beam signal directly at the receiving terminal, lasercom demands highly accurate pointing systems, which can be leveraged to obtain the bearing between the two satellites. Assuming a lasercom crosslink can be established between two satellites, intersatellite bearing can be derived from the as-designed angular offsets between the boresight of the lasercom terminal and the on-board star tracker measuring the spacecraft's inertial attitude.

Long-range RF crosslinks typically cannot be used to similarly derive bearing to the receiving satellite due to the relatively large beamwidth of RF systems. For instance, GNSS satellite antenna half-beamwidths are on the order of 23-26 degrees.[15] In order to measure intersatellite bearing, additional sensors must also be used, such as telescopes or camera/beacon systems. Passive electro-optical sensors are limited by observability constraints that effectively limit the separation between the two satellites in which bearing can be measured. For example, cameras are affected by apparent magnitude and proper illumination of the other spacecraft,[10] and can only work for separations of a few hundreds of kilometers between satellites. Active sensors, such as beacon systems, can be used for longer ranges. Lasercom crosslinks can be considered another form of an active electro-optical system, capable of working over longer ranges.

One major benefit of the proposed concept of intersatellite navigation is that the spacecraft can be operating from wide set of orbits. Satellites can be in the same or similar orbits, such as the proposed mega-constellations in low Earth-orbit (LEO),[16] or they can be in different orbits at different altitudes. For instance, one satellite can be operating in LEO while the other is in geostationary Earth-orbit (GEO). Satellites can be orbiting other central bodies (e.g. Mars), or neutral-gravity points between central bodies (e.g. halo orbits), or entirely separate bodies (e.g. Earth and Mars). In this study, we have chosen to simulate two case studies: (1) an Earth-orbiting scenario, where a GEO relay satellite communicates with satellites in other Earth-orbits, and (2) a Mars-orbiting scenario, where a full satellite constellation is established at Mars with crosslink communication capability.

Key Assumptions

For this study, we assume that all satellites have a lasercom terminal, such as those offered by the company TESAT* or those being developed at MIT,[17] and the accompanying subsystems for power, attitude determination and control (ADC), and command & data handling (C&DH). These systems must operate together in order to establish and maintain a lasercom crosslink between two communicating spacecraft. We assume that crosslinks are established using methods such as performing a scanning maneuver or implementing a coarse beacon system.

Though the narrow beamwidth of lasercom transmission can be used to obtain intersatellite bearing, lasercom also adds some complexity to the communications architecture. The larger beamwidth of RF transmission allows for broadcast signals, which can be transmitted from a single source and received by many, and also typically use low-gain antennas, which can receive signals from a wide range of directions. This simplifies the communications architecture, as it enables satellites to transmit to, or receive from, any other satellites within its antenna's pattern, which is considered a "many-to-many" architecture. Since lasercom transmission uses very narrow beamwidths, it does not easily allow for much beyond point-to-point communications architectures. While this does not present any issue for analysis cases consisting of two satellites, it does introduce complexity in situations of more than two satellites.

In analysis cases of more than two satellites, we designate a certain type of satellite in the constellation as a "hub" satellite that is able to perform simultaneous crosslink communications with all other satellites (the "nodes"). Therefore, the nodes do not crosslink with one another and only communicate with the hubs. We make the assumption that a hub satellite is more complex than the other satellites, and is capable of achieving multiple crosslinks by some means for a "one-to-many/many-to-one" bidirectional association. Simulation of other associations are not in the scope of this paper and are discussed in future work.

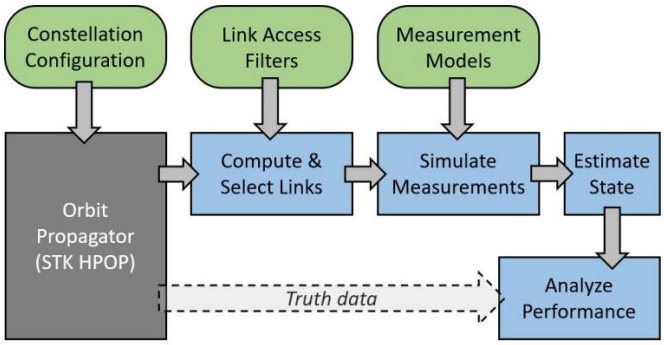

Figure 1. Overview of Simulation Approach. Green ovals indicate inputs. Blue boxes indicate written functions. The gray box indicates an external software/function.

* TESAT Laser Portfolio: http://www.tesat.de/en/products/laser-products

Simulation and Estimation

The simulation environment used for this study is developed in Matlab using satellite state inputs from the High-Precision Orbit Propagator (HPOP), licensed under the AGI Systems Tool Kit (STK) software package. A diagram of the simulation environment is shown in Figure 1.

The orbit propagator is used to generate "truth" data comprised of state vectors (time series of position and velocity) for all satellites within a given constellation case, as configured by the user to emulate existing or proposed satellite mission orbits. In order to match the dynamics model of the estimator, the HPOP force model properties were configured for only J2 perturbation effects. This configuration allows us to evaluate the performance of the enhanced precision and availability of measurements, and not the accuracy of the estimator dynamics model. Test cases have shown that this simpler configuration is consistent with the results of using higher-fidelity models matched in the propagator and estimator, and simply saves computation time.

Link measurement opportunities are computed using the propagated truth data. At each time step, each pair of satellites is evaluated for availability of link access based on geometry, with consideration of filtering parameters such as minimum altitude (effects due to planetary atmosphere), minimum or maximum range (effects due to lasercom capability), and minimum duration (effects due to geometry). In the future, these filters can also include keep-out zones for background objects like the sun, planets, or moons. For this study, we have set all filtering parameters to zero, such that data-gaps are strictly based on geometric occlusion caused by the nearest central body.

Using the state vector and link access-time products from orbit propagation and link computation, respectively, the relative position vector is computed for each link at each time step. The true range measurement is simply the magnitude of the relative position vector. The true bearing is captured by two angles, right ascension and declination in inertial space, from the observing spacecraft to the other. All measurements are then supplied zero-bias Gaussian white noise, based on their respective uncertainty values. In this paper, we assume 3-m range uncertainty (σ_r) to represent RF systems (consistent with literature[10,13]), and a conservative value of 10-cm uncertainty to represent ranging using lasercom systems. The precision of the bearing measurement is typically limited by the uncertainty of the star tracker. In this paper, we assume 2-arcsec bearing uncertainty (σ_b) based on the expected performance of satellite star trackers currently in development.[*]

The simulated observations are then fed into the estimator, which is the extended Kalman filter (EKF) algorithm for intersatellite state estimation as described by Xiong, Wei, and Liu.[10] This incorporates an efficient dynamics model based on the two-body gravity model with J2-perturbations. Other forces, such as atmospheric drag, solar radiation pressure, third-body effects, and additional gravity-mass effects, are not modeled in this estimator. During data-gaps (based on filtering parameters and planetary occlusion), when crosslinks are not available, affected measurements are dropped from the filter's observation model, and the state is estimated based on any measurements that are available, or simply propagated from the most recent state estimate in the case of no measurements being available.

The results from the estimator are then analyzed for performance against the original truth data. We perform a Monte Carlo analysis (N=50) in order to sample noise/uncertainty variations and obtain statistical results. Results are displayed in all figures as the 50th percentile of these Monte Carlo simulations. The main metric used for analysis is the "total position error", which is

[*] Terma Infosheet: T1 & T2 Star Trackers rev2, https://www.terma.com/media/437079/t1_t2_star_tracker_rev2.pdf.

simply the L2 norm of the difference between the estimated and true position vectors. The root-mean-square error (RMSE) is then computed based on the results in the final 10% of the simulation period.

The simulation period is a full day from 04 Apr 2019 16:00:00 to 05 Apr 2019 16:00:00 UTC. All simulation and estimation is performed in the "True of Epoch" coordinate system, with the epoch of 04 Apr 2019 16:00:00. This coordinate system was chosen because it is non-rotating (inertial) and shares the same Z-axis as the Fixed coordinate system, which simplifies computation for gravity terms like J2 in the estimator dynamics model. The initial uncertainty in the position and velocity of each spacecraft is assumed to be 1000 meters and 1 m/s, respectively. Process noise is assumed to be 2e-5 meters in position and 1e-4 meters/sec in velocity.[10]

GEO RELAY CASE STUDY

This analysis is based on NASA's plans for GEO optical relay terminals capable of transmitting data over high-speed crosslinks and downlinks. This technology is expected to primarily serve users in LEO, though it could also be an asset for other Earth-orbiting missions in higher altitudes or highly-elliptical orbits. Two satellites are simulated for this analysis, one each in LEO and HEO.

Table 1. Orbital Parameters for GEO Relay Case Study.

Parameter	GEO	LEO	HEO
a (km)	42442	6945	97462
e	6.12e-4	1.77e-3	9.11e-1
i (deg)	13.3	97.9	7.8
ω (deg)	76.4	317.7	17.7
Ω (deg)	26.8	190.5	112.3
θ (deg)	108.5	42.3	76.0

The GEO and LEO satellite orbits are modeled after the ESA Artemis and JAXA OICETS satellites, respectively, which conducted the first demonstration of a bidirectional intersatellite link in 2005.[18] The HEO satellite orbit is modeled after the four spacecraft of NASA's Magnetospheric MultiScale (MMS) mission, launched in 2015 into a highly elliptical orbit with perigee and apogee at 1.2 and 12 Earth radii, respectively.[19] The orbital parameters of each satellite at simulation epoch are shown in Table 1.

Three scenarios are evaluated within this relay configuration. The first case (a) involves the GEO relay satellite performing crosslink communications with the LEO user terminal only. The second case (b) involves the GEO satellite communicating with the HEO user terminal only. The third case (c) combines the first two cases such that the GEO relay satellite is able to concurrently perform crosslink communications with both user terminals, one in LEO and one in HEO. This case is simulated in order to see if the combined estimation improves performance for one or all of the spacecraft. GNSS receivers represent the current state-of-the-art for satellite positioning and navigation for Earth-orbiting missions, and are therefore chosen as the benchmark for performance comparisons in this analysis.

Case (a): User Terminal in LEO

The GEO and LEO satellites are in view of one another approximately every 90 minutes, resulting in 17 total crosslinks or measurement periods over the simulated day. The separation between the two spacecraft varies between approximately 35,000 and 45,000 kilometers.

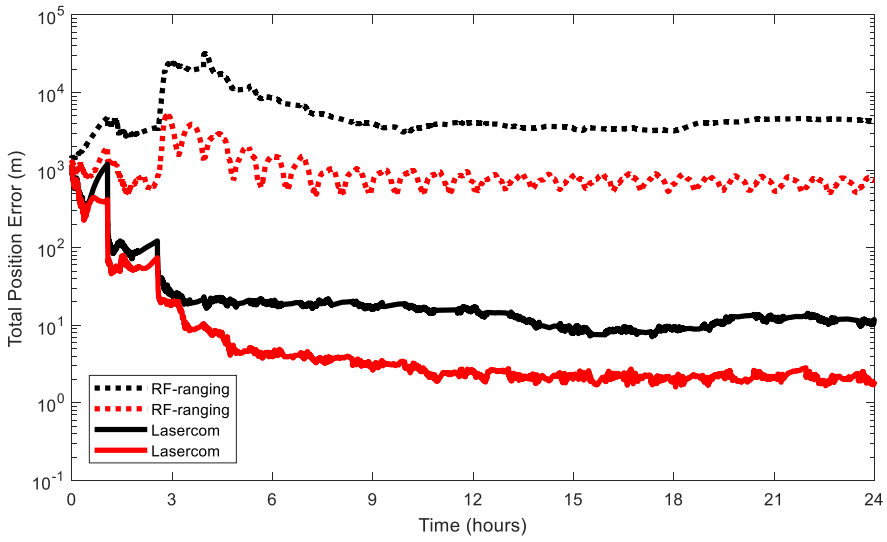

Figure 2. Total Position Error for a GEO Relay with a LEO User Terminal. Results are shown as the 50th percentile values over 50 total simulation runs.

Figure 2 shows the resulting positioning performance for case (a) GEO-LEO over a 24-hour simulation period for two measurement scenarios: (1) range-only from an RF crosslink (in dashed lines), which represents the capability shown in literature for large separations, and (2) range with bearing from a lasercom crosslink (in solid lines), which represents the new capability of our proposed concept. The total position error is shown as a function of time for both the GEO relay satellite (in black) and the LEO user terminal (in red).

The result of the geometric availability of a link between the GEO and LEO satellites, due to Earth-occlusion, can be seen in the error over time. When the LEO satellite is occluded from view of the GEO satellite, the position error steadily increases due to the lack of a new update to the state estimate. One clear example of this occurs on the left side of the figure, from $t \approx 0.3$ to $t \approx 1$ hours, which is about half of the LEO satellite's orbit period, as would be expected. When the LEO satellite returns in view of the GEO satellite from Earth-occlusion, a refined position estimate can be made based on the new measured data, thus replacing the stale estimate from before. This results in a sudden and sharp decrease in error, such as at $t \approx 1$ hour. Another example of this can be seen at $t \approx 2.5$ hours.

Table 2. RMSE of total position error for the GEO-LEO case under two measurement scenarios, where σ_r and σ_b represent the range and bearing 1-sigma uncertainties, respectively.

Scenario	GEO Satellite (m)	LEO Satellite (m)
RF ranging σ_r = 3.0 m	4494	679
Lasercom σ_r = 0.1 m σ_b = 2.0 arcsec	12.0	2.2

As expected, the error in all cases begins near the initial uncertainty value of 1000 meters. From there, however, there is sharp contrast between the results of the lasercom-based measurments, which converge to a better result, and the RF-ranging model, which diverge toward a less certain result. RMSE values of the final results after a 24-hour period of simulation are shown in Table 2. This clearly shows a large improvement (over two orders-of-magnitude) due in part to the increased precision of optical ranging, but more importantly from the availability of bearing measurements at long ranges. Without a directional component, the RF-ranging results show difficulty in accurately estimating the satellites' orbits.

Low-earth orbit satellites are within the primary service volume of GNSS, thus receivers in LEO have been shown to achieve accurate real-time navigation performance within 2-5 meters in total positioning error.[20] Geosynchronous orbits are outside of the GNSS primary service volume, but there have been limited cases of satellites equipped with GNSS receivers, which have been shown to perform within 10-30 meters in total positioning error.[21] As can be seen in Table 2, the proposed lasercom crosslink approach for intersatellite navigation has demonstrated on-par performance with current GNSS technologies for both satellite orbits in this scenario.

Case (b): User Terminal in HEO

The GEO and HEO satellites are in view of one another during the entire period of the simulated day, resulting in continuous measurements (i.e. zero data-gaps) other than the 10-second time-step intervals. The separation between the two spacecraft varies between approximately 120,000 and 226,000 kilometers.

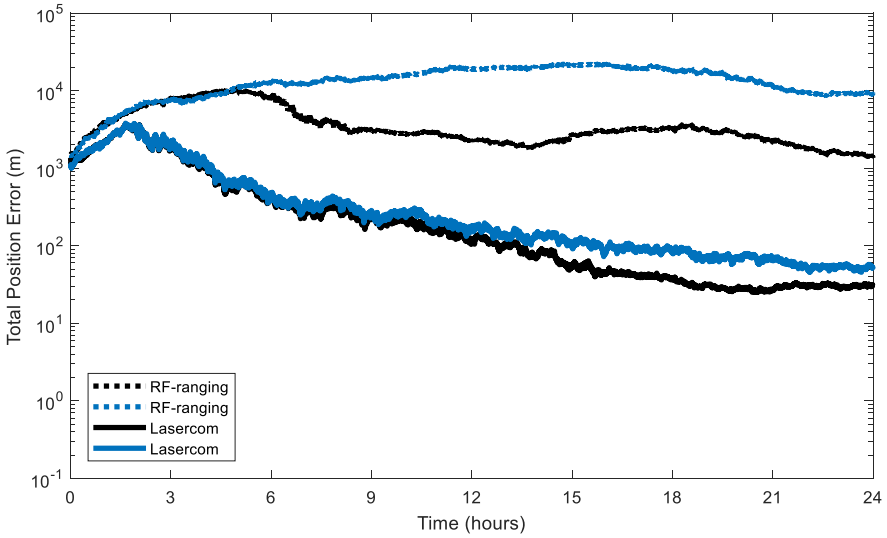

Figure 3. Total Position Error for a GEO Relay with a HEO User Terminal. Results are shown as the 50th percentile values over 50 total simulation runs.

Figure 3 shows the resulting positioning performance for both the GEO relay satellite (in black) and the HEO user terminal (in blue). The simulation is run under the same two measurement scenarios from before: range-only from an RF crosslink (in dashed lines), and range with bearing from a lasercom crosslink (in solid lines).

Table 3. RMSE of total position error for the GEO-HEO case under two measurement scenarios, where σ_r and σ_b represent the range and bearing 1-sigma uncertainties, respectively.

Scenario	GEO Satellite (m)	HEO Satellite (m)
RF ranging σ_r = 3.0 m	1646	9235
Lasercom σ_r = 0.1 m σ_b = 2.0 arcsec	30.6	53.2

Compared to the previous GEO-LEO case, there is less of a difference between the two measurement scenarios, though the lasercom scenario again clearly performs better than RF ranging over time. RMSE values of the final results after a day's worth of continuous observation are shown in Table 3. The performance of the GEO satellite differs in this case from the GEO-LEO case earlier. Although it performs slightly better in the RF-ranging scenario, it does slightly worse in the lasercom scenario. We hypothesize that this is due to the relative geometry of the two satellites in this scenario compared with the previous, but this requires more investigation in future

work. Nonetheless, both the GEO and HEO satellites are able to achieve positioning errors in the tens of meters using lasercom-based intersatellite measurements.

Highly-elliptical orbits are outside of the GNSS primary service volume, but the MMS mission demonstrated a new class of high-altitude GNSS receivers, which were shown to perform within 25-150 meters in total positioning error.[19] The large variation is due to the variable availability of adequate GNSS signals over time. As can be seen in Table 3, the proposed lasercom crosslink approach for intersatellite navigation has demonstrated on-par performance with current GNSS technologies for high-altitude and highly-elliptical orbits.

Case (c): Concurrent Users in LEO and HEO

In this case, the GEO relay satellite is able to perform crosslink communications (and subsequently collect intersatellite measurements) with both the LEO and HEO user terminals at the same time. The individual data-gaps and spacecraft separations described earlier remain true for the respective user terminals. The estimator has continuous input from the GEO-HEO link for the full simulation period; measurements from the GEO-LEO link are added when they are available.

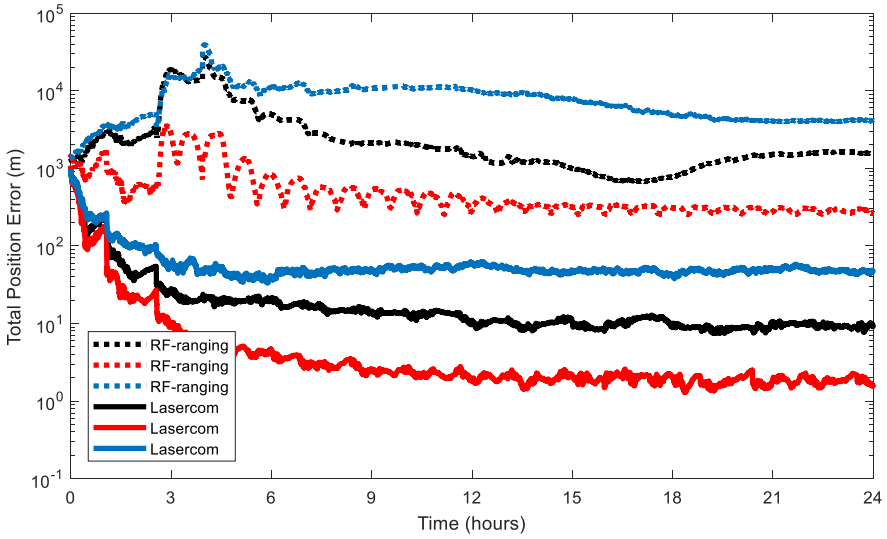

Figure 4. Total Position Error for a GEO Relay and User Terminals in LEO and HEO. Results are shown as the 50th percentile values over 50 total simulation runs.

Figure 4 shows the resulting positioning performance for the GEO relay satellite (in black), the LEO user terminal (in red), and the HEO user terminal (in blue). The simulation is again run under the same two measurement scenarios from before: range-only from an RF crosslink (in dashed lines), and range with bearing from a lasercom crosslink (in solid lines).

Table 4. RMSE of total position error for the combined GEO-LEO and GEO-HEO case under two measurement scenarios, where σ_r and σ_b represent the range and bearing 1-sigma uncertainties, respectively.

Scenario	GEO Satellite (m)	LEO Satellite (m)	HEO Satellite (m)
RF ranging σ_r = 3.0 m	1586	284	4115
Lasercom σ_r = 0.1 m σ_b = 2.0 arcsec	9.4	1.9	48.6

The purpose of running the combined case is to see if the inclusion of both user terminals improves estimation performance for one or all of the spacecraft, such as for the GEO relay satellite since it is the "hub" satellite in this scenario. Based on the RMSE values of the final results in Table 4, this does not seem to be the case. None of the satellites see an appreciable difference in positioning error performance. However, there is a difference in the speed of achieving these results, as demonstrated by comparing the errors of the HEO satellite between Figures 3 and 4. By the 3-hour mark, the HEO satellite in the GEO-HEO case had over 1000-m errors, while the combined GEO relay case shows errors below 100 meters by that same time. The additional link performed between the GEO and LEO satellites allow the GEO satellite to refine its state estimate, which in turn assists in getting higher accuracy estimates of the HEO satellite. Connectivity benefits are an area of future work, to exploit in larger networks of distributed satellites.

MARS CONSTELLATION CASE STUDY

This analysis is based on a Mars-orbiting communication constellation for supporting future human and robotic operations, as proposed by Castellini et al., consisting of six total satellites carrying lasercom payloads for communications with Earth.[22] Although the authors state that crosslink connections would be conducted by radio transmissions, for the purposes of our study, we will assume that they can be performed using lasercom as well.

The constellation is configured as a Walker constellation with the 6 satellites evenly distributed between 2 orbital planes at a constant altitude of 17,030 km and an inclination of 37°. The phase shift between satellites is 5°, and the RAAN separation between orbital planes is 180°. The satellites in the first plane are labeled Sat11, Sat12, and Sat13, while the satellites in the second plane are labeled as Sat21, Sat22, and Sat23.

As we described in our Approach, we demonstrate a framework where a single "hub" satellite in the constellation is able to perform simultaneous crosslink communications with all other satellites (the "nodes"). We consider two scenarios under this framework. In the first, Sat11 is the hub satellite while the remaining satellites are the nodes. In the second, additional hub satellites are implemented. For the RF-ranging case, all satellites are hubs, such that they all can communicate with all others. This is relevant to true capability using RF sensors. For the lasercom case, Sat11 and Sat21 are the hub satellites while the remaining satellites are nodes to both. This is simulated to be a higher-connectivity example of the RF all-to-all case, but reasonably more achievable using lasercom payloads than an all-to-all scenario.

The current method for satellite positioning and navigation for deep-space and Mars-orbiting missions is using radiometric range, Doppler, and very-long baseline interferometry (VLBI)

measurements from the ground-based Deep Space Network (DSN) of global antennas,[23] and is therefore chosen as the benchmark for performance comparisons in this analysis. There have also been studies on using similar techniques, but using optical frequency ground-based antennas instead, that have shown similar performance to current DSN-based positioning.[1,24]

Mars Constellation Results

Each satellite in the constellation is in constant view of all but one of the other satellites within the simulated period of 24 hours. From the perspective of each satellite, its equivalent satellite in the other orbital plane is occluded by Mars twice a day. For Sat11, this occurs with Sat21, resulting in two roughly 10-hour link periods over the simulated day with a 2-hour data-gap in between. Spacecraft separation varies between approximately 15,000 and 41,000 kilometers for non-coplanar satellites, while coplanar satellites have a relatively constant separation of 35,300 kilometers.

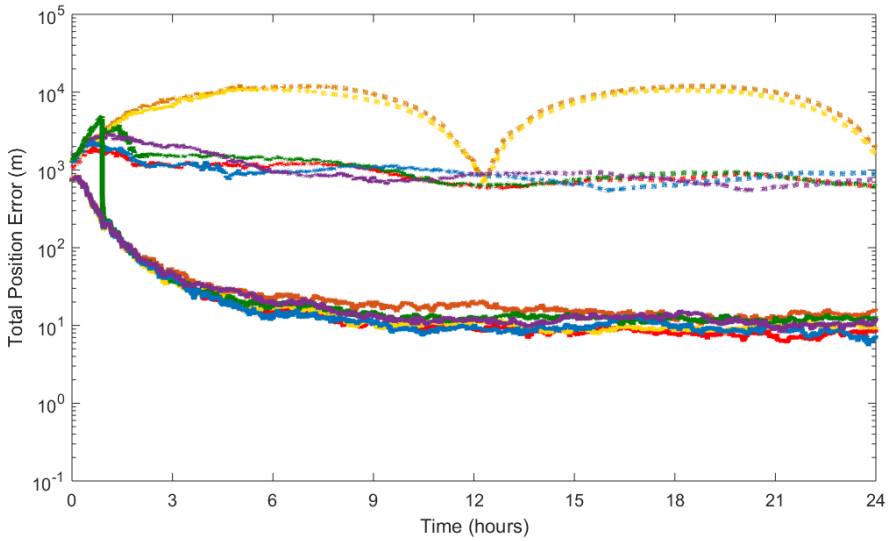

Figure 5. Total Position Error for a 6-Satellite Mars Communications Constellation. The different colors represent the six different satellites, and are used for both measurement scenarios: RF-ranging (dashed) and Lasercom crosslinks (solid). Results are shown as the 50th percentile values over 50 total simulation runs.

Figure 5 shows the resulting position performance over the course of the 24-hour simulation period under the same two measurement scenarios as before: range-only from an RF crosslink (in dashed lines), and range with bearing from a lasercom crosslink (in solid lines). All satellites begin with errors of approximately 1000 meters, due to the initial uncertainty. In the case of RF-ranging, all six satellites generally see no improvement over the course of the simulation. The two satellites in the same plane as the hub satellite demonstrate worse errors than the other four due to the difficulty in resolving orbit position ambiguities with nearly constant range measurements over time.

In the case of lasercom crosslinks, all six satellites have generally the same result, improving over time until about 4 hours into the simulation, after which there are minimal gains in perfor-

mance. The effect of Mars occlusion can be seen in the solid green line (Sat21) at the very beginning of the simulation, from t = 0 to t ≈ 1 hours. The initially poor estimate based on the 1000-meter initial position uncertainty is continuously propagated forward without updates to the state estimate due to the lack of measurements between Sat11 and Sat21. The error continues to grow until about an hour into the simulation, at which point the satellites are in view of one another and a link is established, resulting in a sharp decrease in errors consistent with the other satellites in the constellation.

Table 5. RMSE of total position error for all six satellites in Mars communications constellation. Sat11 is the "hub" satellite than can communicate with all other "node" satellites.

Scenario	Sat11 (m)	Sat12 (m)	Sat13 (m)	Sat21 (m)	Sat22 (m)	Sat23 (m)
RF ranging (1-hub) σ_r = 3.0 m	689	5810	4745	687	908	694
Lasercom (1-hub) σ_r = 0.1 m σ_b = 2.0 arcsec	7.8	14.1	10.1	12.4	7.8	10.4

RMSE values of the final results after 24 hours of observation are shown in Table 5. The results show a large, nearly 100x improvement using lasercom-based measurements for intersatellite navigation over range-only from RF sensors after one day of observation. The proposed lasercom crosslink approach demonstrates absolute positioning errors within 5-20 meters.

McCandless and Martin-Mur performed a study on the navigation performance of a simulated Mars orbiter based on radiometric measurements from the DSN compared with potential optical measurements from a future deep-space optical network.[1] The study showed that both systems achieved comparable results of greater than 25-meter total position errors during periods of active data (roughly two hours each day), and greater than 150-meter errors during data-gaps (roughly 24 hours). As shown in Table 5, the proposed lasercom crosslink approach of intersatellite navigation demonstrates significant improvement, in terms of both spatial and temporal navigation performance, over the current best method of navigating deep-space orbiters.

Table 6. RMSE of total position error for all six satellites in Mars communications constellation. In the RF-ranging case, all satellites can communicate with all other satellites. In the lasercom-case, both Sat 11 and Sat21 are "hub" satellites, while all others are "nodes".

Scenario	Sat11 (m)	Sat12 (m)	Sat13 (m)	Sat21 (m)	Sat22 (m)	Sat23 (m)
RF ranging (All-All) σ_r = 3.0 m	558	522	526	561	563	569
Lasercom (2-hub) σ_r = 0.1 m σ_b = 2.0 arcsec	4.6	5.9	4.4	4.6	5.4	4.8

The results from the "multiple hubs" scenario are summarized in Table 6. In both cases, the modeling of additional hub satellites helps to increase connectivity amongst the satellites, creating a more homogenous set of RMSE values. These values are also slightly better than the best results from the "single hub" scenario presented in Table 5. This result is promising for enhanced performance through means of greater connectivity. We anticipate that developing technologies or strategies for enabling satellites to communicate with any/all other partners, either simultaneously or on a schedule, should see similar gains in navigation performance; these ideas will be investigated in future work.

CONCLUSION

Laser communication crosslinks can support and enable intersatellite range and bearing measurements in order to accurately navigate satellites in GNSS-denied, GNSS-limited, or deep-space environments. Assuming the satellites are equipped with lasercom terminals and the accompanying subsystems to establish crosslinks, distributed satellite systems can leverage connectivity in order to achieve high-accuracy positioning performance, even with initial uncertainty in the other terminal's location. Simulations show lasercom navigation to have on-par performance with GNSS in Earth-orbiting environments, and better performance compared to the current methodology of navigating deep-space orbiters using ground-based ranging and VLBI. The lasercom crosslink method can achieve better positioning performance than DSN-tracking, and also can achieve better temporal performance as it does not suffer day-long data-gaps like DSN.

Future work will include sensitivity studies in order to demonstrate the effects of varying the parameters within the dynamics and measurement models, such as the initial error uncertainty, as well as the effect of intersatellite geometry parameters, such as the size and orbital configurations of constellations. We also will evaluate the effect of higher connectivity among distributed satellites by implementing and analyzing different communications architectures, such as one-to-one, many-to-one, and many-to-many, that can be enabled by new and developing technologies and strategies.

ACKNOWLEDGMENTS

This material is based upon work supported by the United States Air Force under Air Force Contract No. FA8721-05-C-0002 and/or FA8702-15-DO001. Any opinions, findings, and conclusions or recommendations expressed in this material are those of the author and do not necessarily reflect the views of the United States Air Force.

REFERENCES

[1] S.E. McCandless, and T. Martin-Mur, "Navigation Using Deep-Space Optical Communication Systems", AIAA/AAS Astrodynamics Specialist Conference, 2016.

[2] F.L. Markley, "Autonomous Satellite Navigation Using Landmarks", AAS/AIAA Astrodynamics Specialist Conference, 1981.

[3] G. Shorshi, and I.Y. Bar-Itzhack, "Satellite Autonomous Navigation Based on Magnetic Field Measurements", Journal of Guidance, Control, and Dynamics, vol. 18, no. 4, 1995.

[4] R. Zhang, et al., "Low-Earth Orbit Determination Based on Atmospheric Drag Measurements", AAS/AIAA Astrodynamics Specialist Conference, 2018.

[5] J.E. Riedel, et al., "Deep Space 1 Technology Validation Reports: Autonomous Optical Navigation (AutoNav)", NASA JPL Publication 00-10, No. 1, 1999.

[6] S.I. Sheikh, et al., "Spacecraft Navigation Using X-Ray Pulsars", Journal of Guidance, Control, and Dynamics, vol. 29, no. 1, 2006.

[7] F.L. Markley, “Autonomous Navigation Using Landmark and Intersatellite Data”, AIAA-84-1987, AIAA/AAS Astrodynamics Conference, 1984.

[8] M.L. Psiaki, “Autonomous Orbit Determination for Two Spacecraft from Relative Position Measurements”, Journal of Guidance, Control, and Dynamics, vol. 22, no. 2, 1999.

[9] M.L. Psiaki, “Absolute Orbit and Gravity Determination Using Relative Position Measurements Between Two Satellites”, Journal of Guidance, Control, and Dynamics, vol. 34, no. 5, 2011.

[10] K. Xiong, et al., “Autonomous navigation for a group of satellites with star sensors and inter-satellite links”, Acta Astronautica, vol. 86, 2013.

[11] Y. Ou, et al., “Absolute orbit determination using line-of-sight vector measurements between formation flying spacecraft”, Astrophysics and Space Science, vol. 363, 2018.

[12] X. Zhao, et al., “Performance analysis of autonomous navigation of constellation based on inter satellite range measurement”, Procedia Engineering, vol. 15, 2011.

[13] L. Xu, et al., “An autonomous navigation study of Walker constellation based on reference satellite and inter-satellite distance measurement”, IEEE Chinese Guidance, Navigation and Control Conference, 2014.

[14] M.L. Stevens, et al., “Time-of-Flight and Ranging Experiments on the Lunar Laser Communication Demonstration”, Stanford PNT Symposium, 2015.

[15] D.L. Force, “Individual Global Navigation Satellite Systems in the Space Service Volume”, Institute of Navigation International Technical Conference, NASA/TM-2015-218465, 2013.

[16] I. del Portillo, et al., “A Technical Comparison of Three Low Earth Orbit Satellite Constellation Systems to Provide Global Broadband”, Acta Astronautica, vol. 159, 2019.

[17] M.J. Long, “Pointing Acquisition and Tracking Design and Analysis for CubeSat Laser Communication Crosslinks”, Master’s Thesis, MIT, 2018.

[18] P. Muri, and J. McNair, “A survey of communication sub-systems for intersatellite linked systems and cubesat missions”, Journal of Communications, vol. 7, no. 4, 2012.

[19] L. Winternitz, Autonomous Spacecraft Navigation Using Above-the-Constellation GPS Signals, Space Communications and Navigation (SCaN) Workshop: Emerging Technologies for Autonomous Space Navigation, 2017.

[20] A. Hauschild, et al., “The Navigation and Occultation eXperiment: GPS Receiver Performance On Board a LEO Satellite”, Inside GNSS, 2014.

[21] S. Winkler, et al., “GPS Receiver On-Orbit Performance for the GOES-R Spacecraft”, International ESA Conference on Guidance, Navigation & Control Systems, 2017.

[22] F. Castellini, et al., “A mars communication constellation for human exploration and network science”, Advances in Space Research, vol. 45, 2010.

[23] C.L. Thornton, and J.S. Border, “Radiometric Tracking Techniques for Deep-Space Navigation”, Deep-Space Communications and Navigation Series: Monograph 1, 2000.

[24] R.R. Karimi, et al., “A Performance-Based Comparison of Deep-Space Navigation using Optical-Communication and Conventional Navigation Techniques: Small Body Missions” AIAA/AAS Space Flight Mechanics Meeting, 2018.